Online supplement

Differential cardiovascular effects of nano- and micro-particles in mice: Implications for ultrafine and fine particle disease burden in humans

Marin Kuntic[1,2], Ivana Kuntic[1], Dirk Cleppien[3], Andrea Pozzer[4], David Nußbaum[1], Matthias Oelze[1], Tristan Junglas[1], Lea Strohm[1], Henning Ubbens[1], Steffen Daub[1], Maria Teresa Bayo Jimenez[1], Sven Danckwardt[2,5,6], Thomas Berkemeier[7], Omar Hahad[1,2], Matthias Kohl[4], Sebastian Steven[1,5,8], Albrecht Stroh[3,9], Jos Lelieveld[4], Thomas Münzel[1,2], Andreas Daiber[1,2,5]**

[1] University Medical Center Mainz, Department for Cardiology 1, Molecular Cardiology, Mainz, Germany

[2] German Center for Cardiovascular Research (DZHK), Partner Site Rhine-Main, Mainz, Germany

[3] Leibniz-Institut für Resilienzforschung (LIR) gGmbH, Mainz Animal Imaging Center (MAIC), Mainz, Germany

[4] Max Planck Institute for Chemistry, Atmospheric Chemistry Department, Mainz, Germany

[5] Center for Thrombosis and Hemostasis (CTH), University Medical Center of the Johannes Gutenberg-University, Mainz, Germany

[6] University Medical Center Ulm, Department of Clinical Chemistry, Ulm, Germany

[7] Max Planck Institute for Chemistry, Multiphase Chemistry Department, Mainz, Germany

[8] Division of Cardiology, Goethe University Frankfurt, University Hospital, Department of Medicine III, Frankfurt a. M., Germany

[9] University Medical Center Mainz, Institute of Pathophysiology, Mainz, Germany

* These authors contributed equally and are joint senior authors.

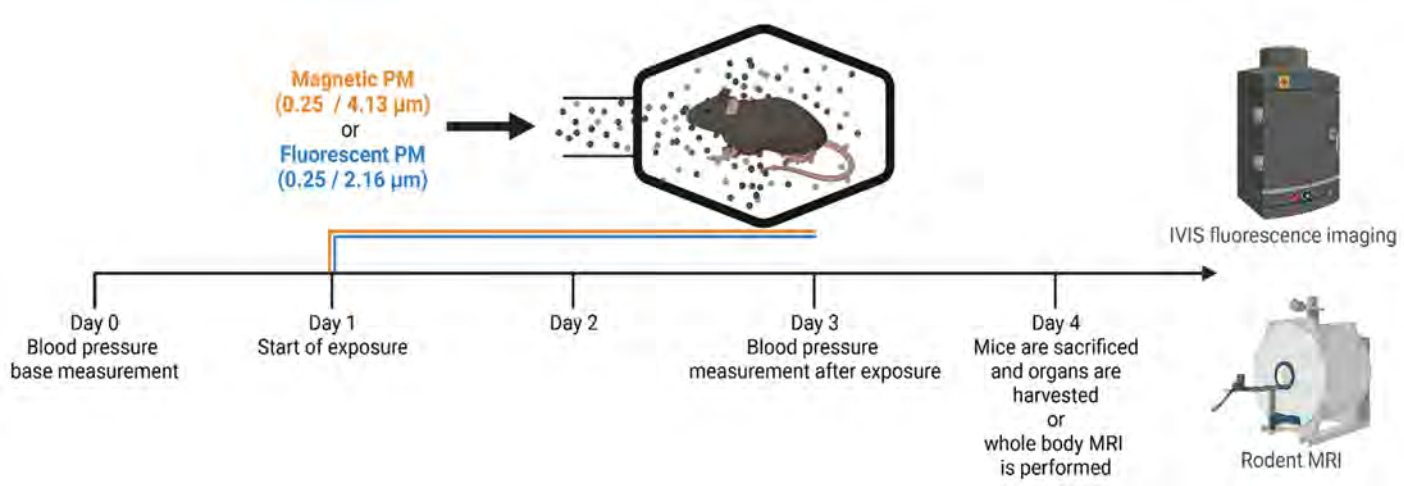

Suppl. Figure S1. Mouse exposure scheme. Mice were exposed to SPM for 3 consecutive days, after which mice were either sacrificed and their organs were harvested for further experiments, including fluorescence imaging, or they were subjected to rodent magnetic resonance imaging. Blood pressure was measured at the baseline and after the final exposure. Created with Biorender.com

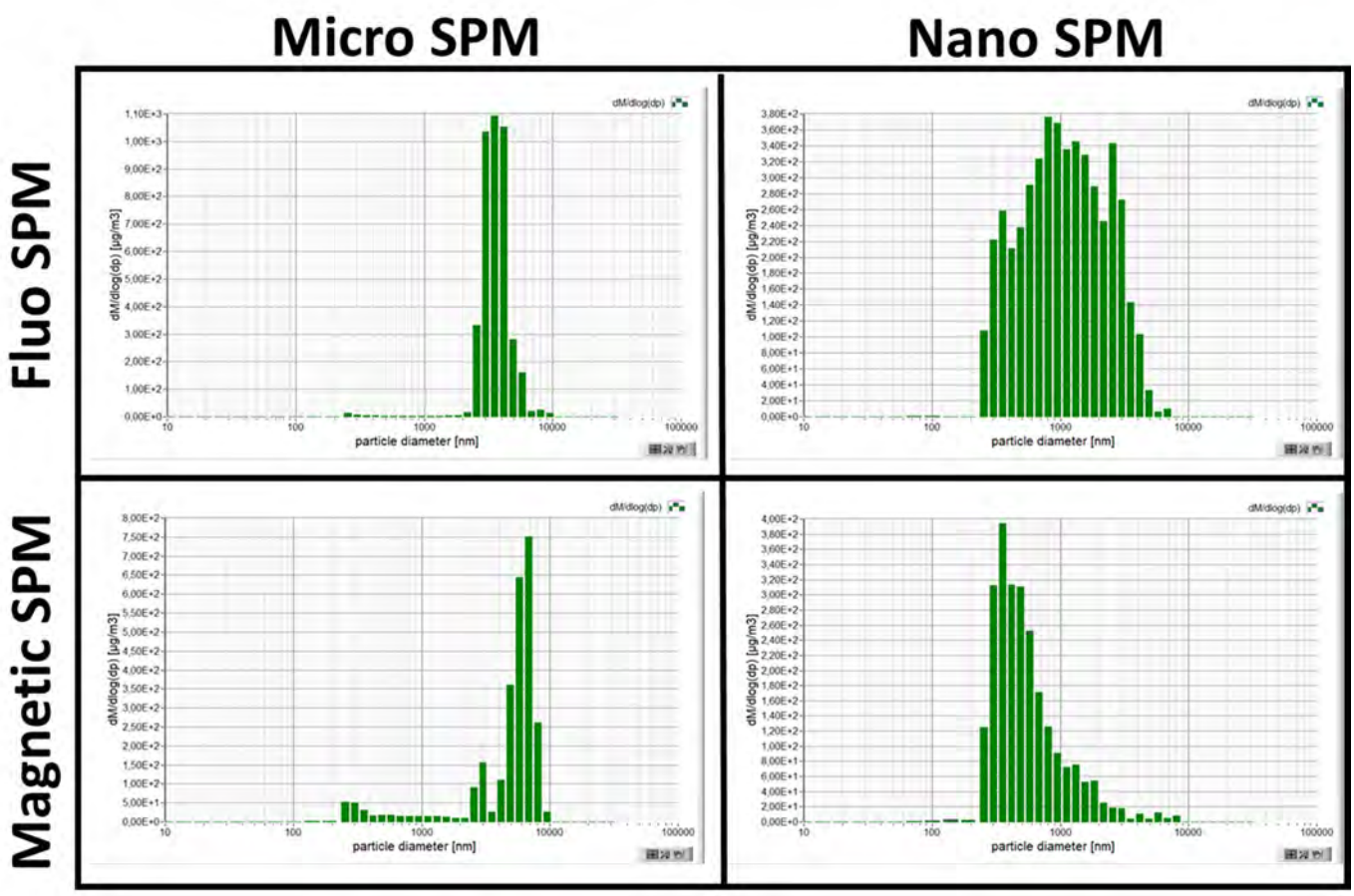

Suppl. Figure S2. Particle size distribution. Representative distributions for all of the different SPM materials used for the experiment, presented as mass distributions. Original diagrams generated by the NanoSpectroPan particle detector.

ONLINE METHODS

Non-invasive blood pressure measurement

Blood pressure was measured using tail-cuff plethysmography with a blood pressure measurement instrument CODA (Kent Scientific, Torrington, CT) [1, 2]. Before the measurement, mice were restrained inside a plastic tube and placed on a preheated plate (32 °C). After a 15-minute rest two cuffs (occlusion cuff and volume pressure recording cuff) were placed on the tail of each mouse. The instrument performs 10 measurement iterations, and the mean is reported. Before the baseline blood pressure measurement was recorded, mice were trained without recording the results at least two times. The final experimental blood pressure (T1) value was recorded after the last exposure to PM.

Isometric tension studies in isolated aortic rings

Aortic ring segments from the thoracic part of the aorta, 4 mm in length, were cleaned from the perivascular adipose tissue and suspended from the force transducers in an organ bath [1, 2]. The force exerted by the aortic rings was measured in the presence of varying concentrations of vasodilators acetylcholine (ACh) and nitroglycerine (GTN) after preconstruction with prostaglandin F2α (yielding approximately 80 % of the maximal tone induced by KCl bolus). Endothelial function was determined by the addition of endothelium-dependent vasodilator, ACh in the range of 10^{-9} to $10^{-5.5}$ M. Endothelium-independent vasodilation was assessed by titrating the pre-constricted aortic rings with GTN in the range of 10^{-9} to $10^{-4.5}$ M. A constant temperature of 37 °C and flow of carbogen gas (95% oxygen, 5% CO_2 v/v) was maintained in the organ chamber throughout the experiment. The cyclooxygenase inhibitor indomethacin (10 μM) was added to the buffer to prevent the production of prostaglandins and other vasoactive eicosanoids that might interfere with the measurement.

Dihydroethidium fluorescence microtopography

Aortic sections from the thoracic part, cortex pieces and lung pieces were embedded in optimal cutting temperature (OCT) compound (TissueTek™, Sakura Finetek, Umkirch, Germany) and snap frozen in liquid

nitrogen [3, 4]. The frozen blocks containing tissue pieces were cut on a cryo-microtome at -25 °C and thickness of 8 µm, transferred onto SuperFrost® (VWR International, Darmstadt, Germany) microscopy slides and stored at -80 °C. The tissue-containing slides were incubated with 1 µM dihydroethidium (DHE) for 30 minutes at 37 °C, washed twice with PBS, protected with a cover slide, and imaged under a fluorescence microscope (Axiovert 40CFL with Axiocam MRm, Zeiss, Germany). The excitation wavelength was set to 510 – 520 nm, and red fluorescence was recorded (emission: 580 – 610 nm). The fluorescence images were quantified as the mean pixel intensity obtained from the area of interest (endothelium and media for the aorta and whole image for lung and cortex) using ImageJ software.

Western blot analysis

Protein expression in tissues of interest was determined by a standard western blot analysis [1, 5]. Protein samples were analyzed using specific primary antibodies against endothelial NO-synthase (eNOS, 1:1000, BD Bioscience #610297, USA), endothelin-1 (ET-1, 1:1000, mouse monoclonal, SantaCruz #sc-517436, Dallas, USA), NADPH oxidase subunits gp91phox (NOX2, mouse monoclonal gp91phox, 1:500, BD Biosciences #611415, USA)), NOX1 (rabbit polyclonal, 1:500, Abcam #ab131088, Cambridge, MA, USA), p67phox (1:1000, BD Bioscience #610913, USA) and phosphorylated p47phox (Neutrophil Cytosolic Factor 1 (NCF-1), 1:000, AssayBiotech #A1161, Sunnyvale, CA), myristoylated alanine-rich protein kinase C substrate phosphorylated at Ser152/156 (P-MARCKS, 1:1000, Cell Signaling, Danvers, MA), cluster of differentiation 68 (CD68, 1:1000, Abcam #ab31630, Cambridge, MA, USA), Manganese superoxide dismutase (MnSOD (SOD-2), 1:1000, Millipore #06-984, Lake Placid, NY), protein kinase Cα1 (PKCα1, 1:5000, BD Bioscience #610107, USA), monocyte chemoattractant protein 1 (MCP-1, 0.4 µg/mL, BioRad #AAM43, Feldkirchen, Germany), heme oxygenase 1 (HO-1, 1:250, Abcam #ab68477, Cambridge, MA, USA), dihydrofolate reductase (DHFR, 1:500, Novus Biologicals, Littleton, CO), and α-actinin or β-actin (1:2500 each, Sigma-Aldrich #A5044 and #A5060, St. Louis, MO) for normalization against loading and transfer. Horseradish-peroxidase conjugated anti-mouse or anti-rabbit were used as secondary antibodies (1:10000 each, Vector Lab. #PI-2000 (anti-mouse IgG) and #PI-1000 (anti-rabbit IgG), Burlingame, CA). Densitometric quantification of antibody-specific bands was performed with an ECL Chemostar Imager (Intas Science Imaging Instruments GmbH, Germany) and Gel-Pro Analyzer software.

LIMITATIONS OF THE STUDY

During the study, we noticed several limitations regarding PM exposure studies in general and the current exposure protocol in particular. One of the major hurdles in assessing the effects of PM with different sizes is the concentration and size distribution. As most of the PM is not uniform in size but follows a certain distribution (e.g. Gaussian), it is quite challenging to achieve a precise exposure concentration (mass flow in $\mu g/m^3$ or particle flow in N/m^3). The difficulty arises because larger particles carry disproportionately more mass than small particles, and mass concentration is the usual way of defining PM concentration, making it highly dependent on the larger particles (mass distribution showed in **Figure S2**). The opposite is true for the number distribution, as smaller particles are more abundant for the same total mass. Whenever a size distribution of PM exists, it is expected that small PM will accompany PM of a larger average diameter and that large PM will significantly contribute to mass concentration, whereas the particle number is largely based on PM with a smaller average diameter. Therefore, it is difficult to draw conclusions about PM health effects based solely on average PM diameter, especially in light of different penetrating depths and organ distribution.

In our experiments, the low amount of PM available through inhalation was insufficient to produce a clear contrast in the MRI experiments. The amount of PM that entered the mouse through inhalation, calculated to be approximately 40 – 120 µg/kg, was at least one order of magnitude lower than the lowest literature values for human contrast applications, where the lower limit is roughly 1000 µg/kg [6, 7]. In addition, this approximated amount of PM is calculated for a whole 6-hour exposure session per day, and the clearance, which can vary greatly, was not taken into account [8]. The larger amount of PM needed for an optimal MRI contrast would require an unrealistically high exposure concentration of more than 2000 $\mu g/m^3$, leading to questionable exposure conditions regarding real-world scenarios. The only way this could be mitigated in the future is through longer exposure time, resulting in the potential accumulation of magnetic particles in the liver, heart, spleen, or brain, where it is taken up by the resident macrophages [9]. However, there are high uncertainties due to not well-characterized clearance processes in healthy mice and differences in particle coating (silica vs. PEG vs. polystyrene), as some studies imply fast clearance in a matter of days [10, 11], and others have observed almost no clearance after as long as 28 days [12] or even 6 months [13].

We attributed the absence of the accumulation of fluorescent nano-sized SPM in the lung of exposed mice to their transmigration into the circulation. However, because exhaled particles were not measured in the present study, the lung's lack of a pronounced fluorescence signal could be due to the reported higher exhalation rate of nanoparticles [14]. Despite this limitation and uncertainty, the assumption of transmigration of nano-sized SPM through the lung was further supported by the present observation of an accumulation of magnetic nanoparticles in the liver by trend. Also, the more pronounced effects of nano-sized SPM compared to microparticles on functional parameters, e.g. blood pressure increase, and oxidative stress parameters and markers of inflammation in remote organs such as the aorta, heart and brain point towards more efficient transmigration of nanoparticles through the lung. These assumptions are also in accordance with human data on the association of UFP exposure with cardiovascular but not respiratory disease risk [15-17] and reported direct effects of nanoparticles on the brain of mice and humans [18-20].

EXTENDED REFERENCES

1. Munzel, T.; Daiber, A.; Steven, S.; Tran, L. P.; Ullmann, E.; Kossmann, S.; Schmidt, F. P.; Oelze, M.; Xia, N.; Li, H.; Pinto, A.; Wild, P.; Pies, K.; Schmidt, E. R.; Rapp, S.; Kroller-Schon, S., Effects of noise on vascular function, oxidative stress, and inflammation: mechanistic insight from studies in mice. *Eur Heart J* **2017,** *38*, (37), 2838-2849.
2. Kroller-Schon, S.; Daiber, A.; Steven, S.; Oelze, M.; Frenis, K.; Kalinovic, S.; Heimann, A.; Schmidt, F. P.; Pinto, A.; Kvandova, M.; Vujacic-Mirski, K.; Filippou, K.; Dudek, M.; Bosmann, M.; Klein, M.; Bopp, T.; Hahad, O.; Wild, P. S.; Frauenknecht, K.; Methner, A., et al., Crucial role for Nox2 and sleep deprivation in aircraft noise-induced vascular and cerebral oxidative stress, inflammation, and gene regulation. *Eur Heart J* **2018,** *39*, (38), 3528-3539.
3. Kuntic, M.; Kuntic, I.; Krishnankutty, R.; Gericke, A.; Oelze, M.; Junglas, T.; Bayo Jimenez, M. T.; Stamm, P.; Nandudu, M.; Hahad, O.; Keppeler, K.; Daub, S.; Vujacic-Mirski, K.; Rajlic, S.; Strohm, L.; Ubbens, H.; Tang, Q.; Jiang, S.; Ruan, Y.; Macleod, K. G., et al., Co-exposure to urban particulate matter and aircraft noise adversely impacts the cerebro-pulmonary-cardiovascular axis in mice. *Redox Biol* **2023,** *59*, 102580.
4. Kuntic, M.; Oelze, M.; Steven, S.; Kroller-Schon, S.; Stamm, P.; Kalinovic, S.; Frenis, K.; Vujacic-Mirski, K.; Bayo Jimenez, M. T.; Kvandova, M.; Filippou, K.; Al Zuabi, A.; Bruckl, V.; Hahad, O.; Daub, S.; Varveri, F.; Gori, T.; Huesmann, R.; Hoffmann, T.; Schmidt, F. P., et al., Short-term e-cigarette vapour exposure causes vascular oxidative stress and dysfunction: evidence for a close connection to brain damage and a key role of the phagocytic NADPH oxidase (NOX-2). *Eur Heart J* **2020,** *41*, (26), 2472-2483.
5. Renart, J.; Reiser, J.; Stark, G. R., Transfer of proteins from gels to diazobenzyloxymethyl-paper and detection with antisera: a method for studying antibody specificity and antigen structure. *Proc Natl Acad Sci U S A* **1979,** *76*, (7), 3116-20.
6. Colbert, C. M.; Ming, Z.; Pogosyan, A.; Finn, J. P.; Nguyen, K. L., Comparison of Three Ultrasmall, Superparamagnetic Iron Oxide Nanoparticles for MRI at 3.0 T. *J Magn Reson Imaging* **2023,** *57*, (6), 1819-1829.

7. Lu, Y.; Huang, J.; Neverova, N. V.; Nguyen, K. L., USPIOs as targeted contrast agents in cardiovascular magnetic resonance imaging. *Curr Cardiovasc Imaging Rep* **2021,** *14*, (2).
8. Keselman, P.; Yu, E. Y.; Zhou, X. Y.; Goodwill, P. W.; Chandrasekharan, P.; Ferguson, R. M.; Khandhar, A. P.; Kemp, S. J.; Krishnan, K. M.; Zheng, B.; Conolly, S. M., Tracking short-term biodistribution and long-term clearance of SPIO tracers in magnetic particle imaging. *Phys Med Biol* **2017,** *62*, (9), 3440-3453.
9. Tan, H. H.; Fiel, M. I.; Sun, Q.; Guo, J.; Gordon, R. E.; Chen, L. C.; Friedman, S. L.; Odin, J. A.; Allina, J., Kupffer cell activation by ambient air particulate matter exposure may exacerbate non-alcoholic fatty liver disease. *J Immunotoxicol* **2009,** *6*, (4), 266-75.
10. Zhou, C.; Long, M.; Qin, Y.; Sun, X.; Zheng, J., Luminescent gold nanoparticles with efficient renal clearance. *Angew Chem Int Ed Engl* **2011,** *50*, (14), 3168-72.
11. Alric, C.; Miladi, I.; Kryza, D.; Taleb, J.; Lux, F.; Bazzi, R.; Billotey, C.; Janier, M.; Perriat, P.; Roux, S.; Tillement, O., The biodistribution of gold nanoparticles designed for renal clearance. *Nanoscale* **2013,** *5*, (13), 5930-9.
12. Li, X.; Wang, B.; Zhou, S.; Chen, W.; Chen, H.; Liang, S.; Zheng, L.; Yu, H.; Chu, R.; Wang, M.; Chai, Z.; Feng, W., Surface chemistry governs the sub-organ transfer, clearance and toxicity of functional gold nanoparticles in the liver and kidney. *J Nanobiotechnology* **2020,** *18*, (1), 45.
13. Sadauskas, E.; Danscher, G.; Stoltenberg, M.; Vogel, U.; Larsen, A.; Wallin, H., Protracted elimination of gold nanoparticles from mouse liver. *Nanomedicine* **2009,** *5*, (2), 162-9.
14. El-Sherbiny, I. M.; El-Baz, N. M.; Yacoub, M. H., Inhaled nano- and microparticles for drug delivery. *Glob Cardiol Sci Pract* **2015,** *2015*, 2.
15. Meng, X.; Ma, Y.; Chen, R.; Zhou, Z.; Chen, B.; Kan, H., Size-fractionated particle number concentrations and daily mortality in a Chinese city. *Environ Health Perspect* **2013,** *121*, (10), 1174-8.
16. Stolzel, M.; Breitner, S.; Cyrys, J.; Pitz, M.; Wolke, G.; Kreyling, W.; Heinrich, J.; Wichmann, H. E.; Peters, A., Daily mortality and particulate matter in different size classes in Erfurt, Germany. *J Expo Sci Environ Epidemiol* **2007,** *17*, (5), 458-67.
17. Bergmann, M. L.; Andersen, Z. J.; Massling, A.; Kindler, P. A.; Loft, S.; Amini, H.; Cole-Hunter, T.; Guo, Y.; Maric, M.; Nordstrom, C.; Taghavi, M.; Tuffier, S.; So, R.; Zhang, J.; Lim, Y. H., Short-term exposure to ultrafine particles and mortality and hospital admissions due to respiratory and cardiovascular diseases in Copenhagen, Denmark. *Environ Pollut* **2023,** *336*, 122396.
18. Cheng, H.; Saffari, A.; Sioutas, C.; Forman, H. J.; Morgan, T. E.; Finch, C. E., Nanoscale Particulate Matter from Urban Traffic Rapidly Induces Oxidative Stress and Inflammation in Olfactory Epithelium with Concomitant Effects on Brain. *Environ Health Perspect* **2016,** *124*, (10), 1537-1546.
19. Gonzalez-Maciel, A.; Reynoso-Robles, R.; Torres-Jardon, R.; Mukherjee, P. S.; Calderon-Garciduenas, L., Combustion-Derived Nanoparticles in Key Brain Target Cells and Organelles in Young Urbanites: Culprit Hidden in Plain Sight in Alzheimer's Disease Development. *J Alzheimers Dis* **2017,** *59*, (1), 189-208.
20. Haghani, A.; Johnson, R.; Safi, N.; Zhang, H.; Thorwald, M.; Mousavi, A.; Woodward, N. C.; Shirmohammadi, F.; Coussa, V.; Wise, J. P., Jr.; Forman, H. J.; Sioutas, C.; Allayee, H.; Morgan, T. E.; Finch, C. E., Toxicity of urban air pollution particulate matter in developing and adult mouse brain: Comparison of total and filter-eluted nanoparticles. *Environ Int* **2020,** *136*, 105510.